

Short communication

# Preparation and characterization of tin-based three-dimensional cellular anode for lithium ion battery

Tao Jiang<sup>a</sup>, Shichao Zhang<sup>b</sup>, Xinping Qiu<sup>a,\*</sup>, Wentao Zhu<sup>a</sup>, Liquan Chen<sup>a</sup>

<sup>a</sup> Key Lab of Organic Optoelectronics and Molecular Engineering, Department of Chemistry, Tsinghua University, Beijing 100084, China

<sup>b</sup> School of Materials Science and Engineering, Beijing University of Aeronautics and Astronautics, Beijing 100083, China

Received 17 September 2006; accepted 12 January 2007

Available online 18 January 2007

## Abstract

A three-dimensional cellular Sn-based anode has been prepared by electrodepositing tin onto 3D copper matrix under different current conditions and characterized by means of scanning electron microscope (SEM), X-ray diffraction (XRD), electrochemical cycling test. The properties of tin layer, such as particle size, porosity and shape, greatly affect cycling behavior of electrodes. Beside this, two additional factors including large bonding force and three-dimensional stress-alleviated environment are also important to the dimensional stability of electrodeposited layer. In order to improve cycling performance, a composite anode configuration is designed by casting inactive carbon black into the “valley-ridge” tin-coated architecture. Capacity fading of both anodes is remarkably suppressed with the help of mechanical compression coming from stuffing. Taking advantage of the 3D electrode configuration, CTA with stuffing experiences a more uniform diffusion process to form an intermetallic layer of  $\text{Cu}_6\text{Sn}_5$  when heated and shows better cyclicality than 2D annealed anode.

© 2007 Elsevier B.V. All rights reserved.

**Keywords:** Lithium ion battery; Anode; Current collector; Electrodeposition

## 1. Introduction

Although widely used in the field of various portable electric devices as a power supply, lithium ion batteries have still attracted much attention in attempts to ameliorate the performance of their inside components. The conventional anode for lithium ion battery is fabricated by well-known “slurry-coating” technology on flat copper foil, where the slurry consists of active materials, conductive agents and binders. Compared with graphite, some alternative anodic materials such as tin and its alloy usually endure severe volume expansion and contraction during lithiation/delithiation process [1–6]. The electrode cannot accommodate large internal stress stemming from such volume changes, which causes the active materials pulverize and delaminate from copper foil. Consequentially, the performance of electrode degrades rapidly after a few charge/discharge cycles [7–10]. Just because of this, some work has been undertaken to improving anode performance by changing the nature

and morphology of electrodes. Tamura et al. [11] firstly fabricated a new type of electrode by electrodepositing Sn on Cu foil and subsequent annealing. They also proved that the rough surface of copper foil is beneficial to the integrality of electrodes, and the improving cyclability is mainly attributed to a micro-columnar structure of the deposits [12]. Simultaneously, some three-dimensional substrates, such as carbon paper, nickel foam, etc. [13–15], were used as current collectors to enhance the cycle life of various active materials. The 3D matrix offers such a good conductive environment that the active materials can be stuck to the current collector without addition of conductive agents; it can also relieve the stress due to the volume changes and then impede failure of electrodes. Thus, seeking an ideal structure of the current collector suitable for those new anode materials with higher capacity seems to hold the key to putting them into commercial application ultimately.

Recently, we have developed a method of fabricating three-dimensional copper cellular architecture (seen in Fig. 1) by multiplestep electrodeposition without any polymer framework based on Shin’s work [16,17]. Subsequently, an electrochemical study was conducted using electrodes prepared by filling graphite–silicon mixture into the 3D copper matrix acted as

\* Corresponding author. Fax: +86 10 62794234.

E-mail address: [qiuxp@mail.tsinghua.edu.cn](mailto:qiuxp@mail.tsinghua.edu.cn) (X. Qiu).

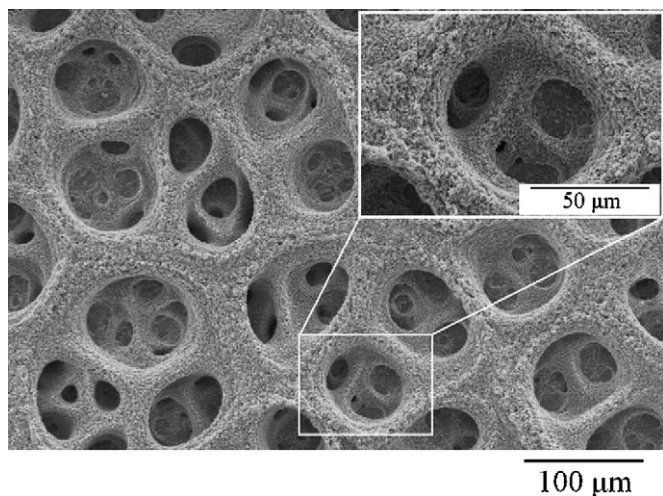


Fig. 1. SEM images of 3D copper cellular architecture fabricated by electrodeposition.

current collector. The excellent performance indicates that the unique anode design has attractive potential in further research of advanced anode for lithium ion battery. Moreover, other active materials just like Sn and its alloy can be reappraised based on this novel 3D cellular copper.

In this article, a kind of Sn-based three-dimensional cellular anode is prepared by electrodeposition under different current conditions and subsequent heat treatment. In order to evaluate the effect of mechanical compression on the cycling behavior, a composite anode is designed by casting inactive carbon black into the “valley-ridge” Sn-coated architecture. The electrochemical properties and failure causes of these electrodes are respectively presented and discussed.

## 2. Experimental

The 3D Sn cellular anodes were prepared by electrodepositing tin onto 3D copper matrix using the bath described in Table 1 under two conditions: (i) constant current of  $50 \text{ mA cm}^{-2}$  for 240 s; (ii) pulsed current of  $0.3 \text{ A cm}^{-2}$  for 100 s, whose frequency is 200 Hz with an on/off ratio waveform of 1:1. Tin plate was used as anode and the electrolytic solution was continually circulated through a pump, the working temperature of both steps was  $25^\circ\text{C}$ . A composite electrode was fabricated by filling slurries of 90 wt% carbon black and 10 wt% polyvinylidene fluoride (PVDF) dissolved in *N*-methylpyrrolidinone (NMP) into electrodeposited cellular Sn architecture. Carbon black powders have an average particle size of 50 nm. The electrodes were dried and compressed under pressure of 6 MPa, then redundant mix-

Table 1  
Composition of the electrolytic solution for tin electrodeposition

Materials	Concentration
$\text{SnSO}_4$ ( $\text{mol l}^{-1}$ )	0.15
$\text{H}_2\text{SO}_4$ (98%) ( $\text{mol l}^{-1}$ )	1.5
Addition agent <sup>a</sup> ( $\text{ml l}^{-1}$ )	20

<sup>a</sup> Produced by FengFan Co. Ltd., Wuhan, China.

ture on electrodes was scraped off to make the filling materials not higher than top of the 3D structures. All of the electrodes were dried at  $60^\circ\text{C}$  in vacuum before using. The heat treatment was conducted at  $210^\circ\text{C}$  for 24 h in vacuum.

The electrochemical characterizations were performed using coin cells. Test cells were assembled with electrodes ( $0.8 \text{ cm} \times 0.8 \text{ cm}$ ), lithium foil and polypropylene separators in an Ar filled glovebox. A 1.0 M  $\text{LiPF}_6$  solution in a 1:1 vol.% mixture of ethylene carbonate (EC) and diethyl carbonate (DEC) was used as the electrolyte. All cells were cycled at a constant current of  $0.1 \text{ mA mg}^{-1}$  between 20 mV and 2.0 V.

X-ray diffraction (XRD, MAC Science, Cu  $\text{K}\alpha$ , 40 kV, 40 mA) was used to determine crystal phases and average grain size of deposits. The surface and cross-section morphology was observed by aids of scanning electron microscope (SEM, KYKY-2800).

## 3. Results and discussion

Fig. 2(a)–(d) shows the top and cross-section micrographs of electrodeposited Sn 3D cellular anodes prepared under two current conditions. The copper matrix was homogeneously covered by tin layer wherever on “valleys” or “ridges”. Average thickness of both metallic layer was about  $3 \mu\text{m}$ . Due to the dissimilar fabrication process, two electrodes have shown obvious differences in morphology and other characteristics (shown in Table 2). Tin anode electrodeposited at low current density has a smooth surface and compact structure. There is a perceptible crevice between the copper substrate and above tin layer; by contrast, tin anode electrodeposited at high current density has a relatively rough surface and loose structure resulted from hydrogen evolution at large overpotential. Similarity in configurations of the tin layer and copper substrate makes it difficult to distinguish the interface between them from SEM images. In addition, the 3D configuration has an important advantage compared with conventional 2D one. The calculated area density of tin layer with the same thickness of  $3 \mu\text{m}$  on a flat copper foil is about  $2.19 \text{ mg cm}^{-2}$ . This result is much smaller than  $4.31 \text{ mg cm}^{-2}$  of the 3D compact tin anode (CTA) demonstrated in Table 2. That means the 3D electrode can achieve large area energy capacities without making any sacrifices in thickness of active materials, and the thicker tin layer is inimical to electrode performance because of increased ohmic resistance, longer Li ion transport distance and relevant capacity loss [18]. Due to the porous characteristic, area density of loose tin anode (LTA) is  $1.84 \text{ mg cm}^{-2}$ , about 16% lower than above calculated result. Fig. 2(e) and (f) shows the SEM micrographs of CTA filled with carbon black. Copper framework is kept intact except being slightly planished

Table 2  
Characteristics of two tin cellular anodes electrodeposited under different current conditions

	Grain size <sup>a</sup> (nm)	Tin area density ( $\text{mg cm}^{-2}$ )
Compact tin anode	480	4.31
Loose tin anode	120	1.84

<sup>a</sup> Calculated by Scherrer equation.

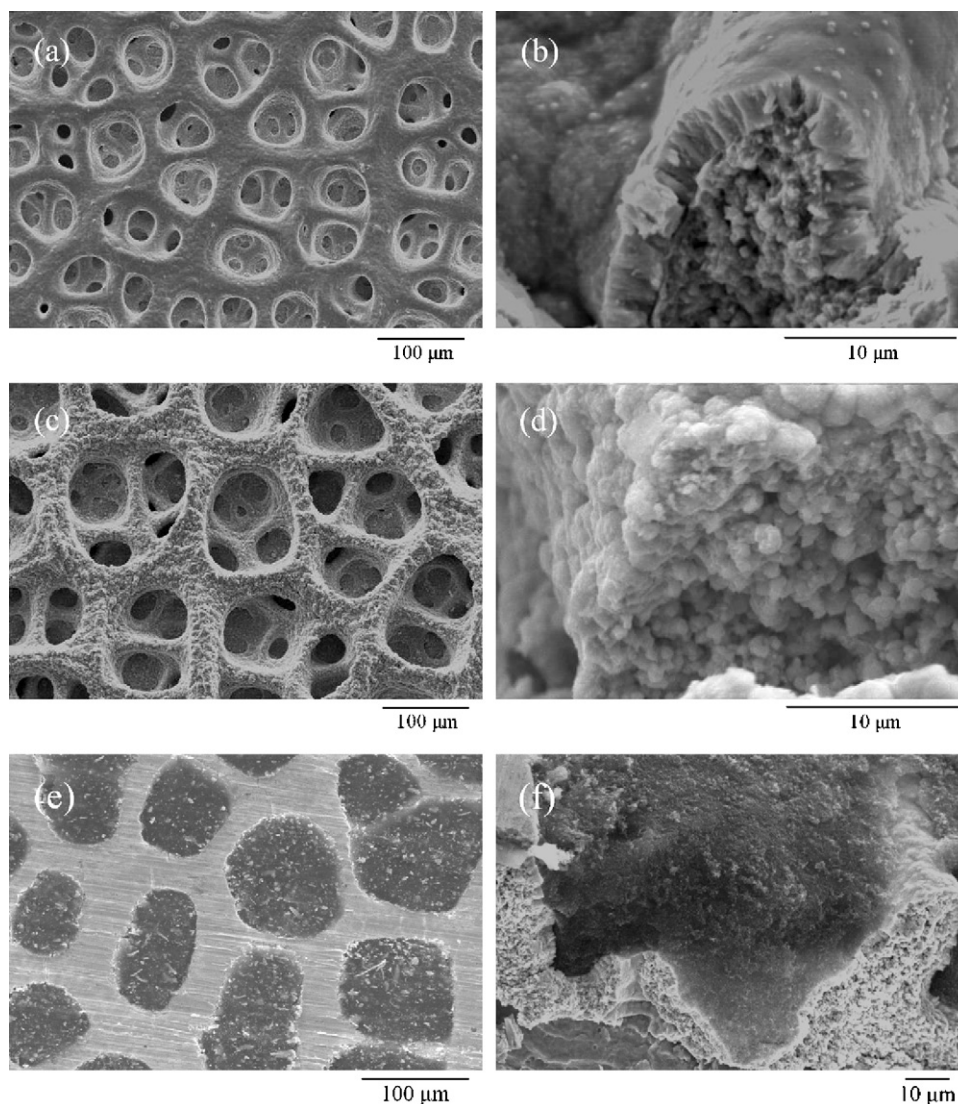


Fig. 2. Top and cross-section micrographs of electrodeposited 3D tin cellular anodes: (a and b) CTA, (c and d) LTA and (e and f) CTA filled with carbon black.

under 6 MPa compression. The stuffing powders are separated to some small cells by walls of 3D architecture. Seen from cross-section of the electrode (Fig. 2(f)), carbon black has been solidly pressed into the micropores and contacted with electrodeposited Sn layer tightly. LTA with similar configurations is not shown here.

The potential profiles of two Sn cellular electrodes without stuffing for the first 1.5 cycles are shown in Fig. 3. During Li insertion process, a slope ranging from 1.6 to 0.8 V appears at initial discharge curve of both samples. This region is related to the decomposition of tin oxide formed after electroplating [9,19]. A long irreversible plateau at about 1.5 V was observed in second discharge curve of the CTA, which is associated with catalytic decomposition of electrolyte and SEI formation according to previous studies [20]. Same reaction happened in the LTA, and it is really interesting that the irreversible capacity of CTA due to such SEI formation seems much higher than that of LTA although LTA is rougher and possesses larger fresh Sn surface that is active for catalytic process. However, this phenomenon

can easily be understood if considering the huge volume changes during initial lithiation/delithiation cycle. As demonstrated in Fig. 4(a), the CTA layer after first cycle was severely destroyed by huge internal stress, and simultaneously generated a great amount of fresh tin surface to react with electrolyte in the second cycle, whereas LTA avoided such damage with the help of its special structure. The plateaus corresponding to formation of  $\text{Li}_2\text{Sn}_5$  and  $\text{LiSn}$  can be clearly seen in the second discharging curve of both electrodes.

The cycling behavior and relevant SEM images of four tin cellular anodes are indicated in Fig. 4. Due to great damage by huge internal stress as shown in Fig. 4(a), the reversible capacity of CTA has rapidly degraded from  $894$  to  $195 \text{ mAh g}^{-1}$  within 20 cycles. In contrast, LTA whose reversible capacity keeps above  $800 \text{ mAh g}^{-1}$  even after 12 cycles shows better performance, which should be mainly attributed to its small grain size and porous structure that can effectively relieve huge internal stress and then impede pulverization and delamination of the host materials [7,21]. The SEM micrograph of LTA provided con-



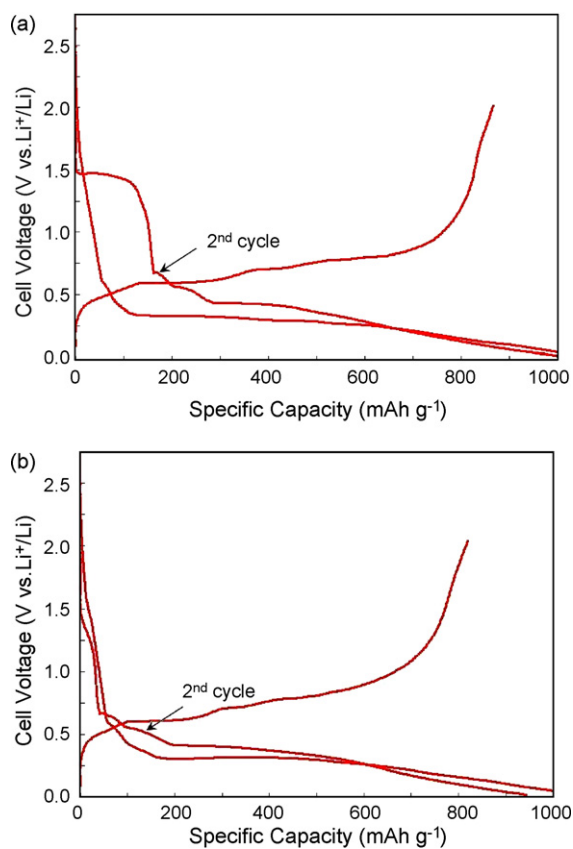


Fig. 3. Potential profiles of (a) compact tin anode and (b) loose tin anode without stuffing.

vincing evidence for this issue by presenting its intact surface after the 10th cycle in Fig. 4(b). Besides this, the contribution of two additional factors for dimensional stability of LTA should not be neglected here. Firstly, the Cu substrate having coarse surface can engage with loose tin layer tightly. Their improved bonding force is helpful to ameliorates the electrochemical performance; secondly, distinguished from conventional flat copper foil, tin layer deposited on 3D copper matrix can swell in a

three-dimensional environment rather than on a plane surface. As a result, the active materials may crack regularly in the place with large curvature where internal stress distributes in different directions (seen in Fig. 4(b)). Such structure characteristic is beneficial to alleviate serious damage to electrodes stemming from periodical volume changes. The reversible capacity of LTA decreased gradually since the 13th cycle and approached to  $460 \text{ mAh g}^{-1}$  when the test terminated. In order to investigate what causes the capacity fading, SEM micrograph of LTA after the 15th cycle was manifested in Fig. 4(c). It can be seen that some bulk tin layer peeled off from side wall of 3D copper substrate, which may be related to the penetration of electrolyte into crevice between tin layer and current collector through cracks. The loss of electronic contacting should be responsible for electrode failure during the last several cycles [7].

In attempt to improve cyclicality of tin cellular anode, a feasible effort could be made to impede delaminating of tin layer from the substrate no matter what the delamination originated from, such as internal stress, low bonding force or electrolyte penetration. From this point of view, a composite anode was designed by casting inactive carbon black powders into the “valley” of 3D tin-coated architecture. For purpose of evaluate these tin cellular anodes more accurately, carbon black is selected as stuffing just because of its excellent conductivity and inert to  $\text{Li}^+$  insertion. The cycle behavior seems different when carbon black powders are pressed into tin-coated matrix. As shown in Fig. 4, capacity fading of CTA was remarkably suppressed, and its reversible capacity remained  $823 \text{ mAh g}^{-1}$  even after the seventh cycle. The phenomenon can be explained that tin layer would crack to smaller particles during charging/discharging process, but it does not peel off and still maintains contact with Cu substrate by aids of the mechanical compression coming from stuffing. In addition, the internal stress due to volume changes of tin layer can be homogeneously dispersed to other cells through around wall of micropores. So the resultant force keeps balance for an integrate cell, which makes the whole composite anode more stable than the samples without stuffing. However, CTA was proved not an ideal choice during the subsequent test. The

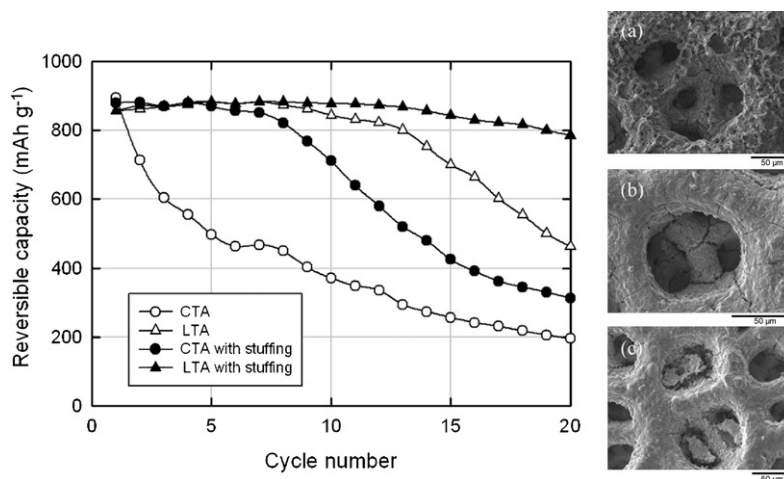


Fig. 4. Cycle performance of four tin cellular anodes and relevant SEM images of (a) CTA after 1st cycle, (b) LTA after 10th cycle and (c) LTA after 15th cycle.

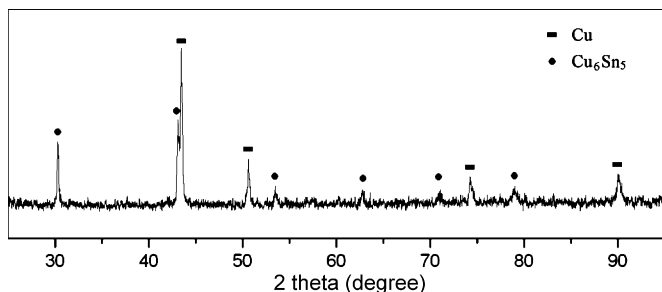


Fig. 5. XRD pattern of CTA filled with carbon black after heat treatment.

incessant pulverization of tin layer and formation of resistive surface films on it result in increased cell impedance. Consequently, the reversible capacity of electrodes degrades rapidly to only  $312 \text{ mAh g}^{-1}$  after the 20th cycle. The similar results on bulk tin have been reported by Yang et al. [19]. Since the 14th cycle, the capacity fading of LTA with carbon black has been obviously slowed down. The mechanical compression in electrodes can effectively prevent tin layer from delaminating resulted from electrolyte penetration and reaction. So the final reversible capacity was greatly improved to  $785.2 \text{ mAh g}^{-1}$  and average coulomb efficiency exceeded 94.2% during 20 cycles. In comparison with previous studies [11,19] relevant to pure tin anode, the result has been remarkably improved by the aid of 3D electrode configurations.

Heat treatment is used to ameliorate cycle life of CTA with carbon black. As XRD pattern shown in Fig. 5, an intermetallic compound of  $\text{Cu}_6\text{Sn}_5$  forms on surface of annealed electrode. Except Cu and  $\text{Cu}_6\text{Sn}_5$ , no other phases are observed just like Sn and  $\text{Cu}_3\text{Sn}$  [11]. Fig. 6(a) shows cross-section micrograph of CTA with stuffing after heat treatment. Compared with original  $3 \mu\text{m}$  tin film, the thickness of alloy layer increases to about  $5 \mu\text{m}$ . Tin and copper diffuse to each other when heated, so the alloy layer adjacent to substrate inherits structure characteristic of 3D copper architecture and seems looser than its upper part. The carbon black has also played an important role during heat treatment. Fig. 6(b) shows the SEM image of annealed CTA without any stuffing at same condition of  $210^\circ\text{C}$  for 24 h. Due to huge stress produced from different coefficient of thermal expansion, the electrodeposited layer will crack and delaminate

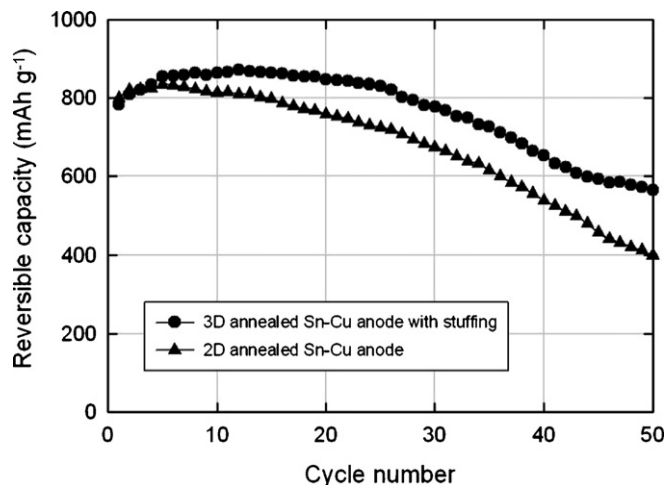


Fig. 7. Comparative cycling performance of annealed 3D and 2D Sn-Cu electrodes.

from copper substrate. By contrast, pressure coming from stuffing can help Sn film contact tightly with current collector and make the diffusion of two elements more uniform.

Fig. 7 shows the electrochemical performance of 3D annealed CTA filled with carbon black. Due to the formation of  $\text{Cu}_6\text{Sn}_5$  that can effectively relieve volume changes of the active layer, annealed anode has a better cyclicality than as-deposited CTA shown in Fig. 4. A comparative result of 2D electrode prepared on copper foil with same tin thickness and anneal conditions has also been shown here. Reversible capacity of CTA has a peak value of  $872 \text{ mAh g}^{-1}$  at the 12th cycle increasing from  $784 \text{ mAh g}^{-1}$  at the first cycle, and gradually decreases to about  $564 \text{ mAh g}^{-1}$  within 50 cycles. However, the capacity retention of 2D electrode after 50th cycle is only  $398 \text{ mAh g}^{-1}$ , about 50% of its initial capacity. As discussed above, the difference of cycle life in two electrodes should be attributed to their configuration. Further work has been done to replace inactive carbon black with other anodic materials just like graphite or silicon. If the walls of copper framework can similarly restrict their volume changes into a cell scale and keep the electrode stable during charging/discharging process, the 3D anode design will have more use in advanced anode for lithium battery.

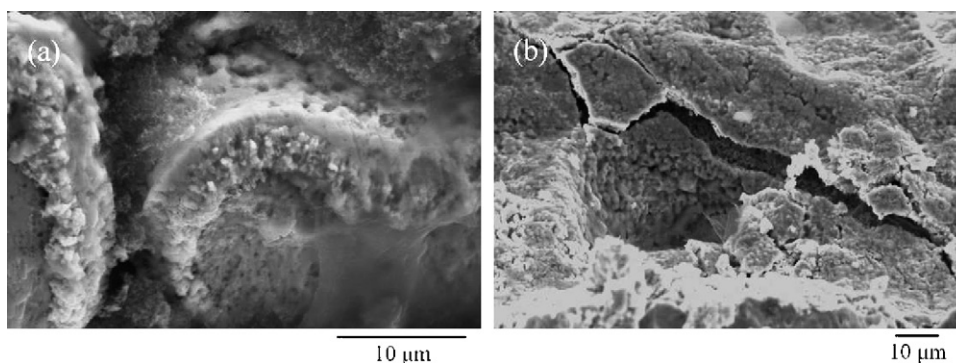


Fig. 6. Cross-section micrographs of annealed CTA (a) with and (b) without stuffing.

#### 4. Conclusions

A three-dimensional cellular Sn-based anode has been prepared by electrodepositing tin onto 3D copper matrix under different current conditions. The properties of tin layer, such as particle size, porosity and shape, greatly affect cycling behavior of electrodes. Beside this, two additional factors including large bonding force and three-dimensional stress-alleviated environment are also important to the dimensional stability of electrodeposited layer. In order to improve cycling performance, a composite anode configuration is designed by casting inactive carbon black into the “valley-ridge” tin-coated architecture. Capacity fading of both anodes is remarkably suppressed with the help of mechanical compression coming from stuffing. Taking advantage of the 3D electrode configuration, CTA with stuffing experiences a more uniform diffusion process to form an intermetallic layer of  $\text{Cu}_6\text{Sn}_5$  when heated and shows better cyclicality than 2D annealed anode.

#### Acknowledgements

This work was supported by State Key Basic Research Program of PRC (2002CB211803) and National Science Foundation of China (50574008 and 9041002).

#### References

- [1] G.X. Wang, J.H. Ahn, J. Yao, S. Bewlay, H.K. Liu, *Electrochem. Commun.* 6 (2004) 689.

- [2] K.D. Kepler, J.T. Vaughey, M.M. Thackeray, *J. Power Sources* 81–82 (1999) 383.
- [3] A.H. Whitehead, J.M. Elliott, J.R. Owen, *J. Power Sources* 81–82 (1999) 33.
- [4] J. Yang, M. Wachtler, M. Winter, J.O. Besenhard, *Electrochem. Solid-State Lett.* 2 (1999) 161.
- [5] H. Li, X.J. Huang, L.Q. Chen, Z.G. Wu, Y. Liang, *Electrochem. Solid-State Lett.* 2 (1999) 547.
- [6] Z.P. Guo, J.Z. Wang, H.K. Liu, S.X. Dou, *J. Power Sources* 146 (2005) 448.
- [7] M. Winter, J.O. Besenhard, *Electrochim. Acta* 45 (1999) 31.
- [8] M. Wachtler, J.O. Besenhard, M. Winter, *J. Power Sources* 94 (2001) 189.
- [9] M. Inaba, T. Uno, A. Tasaka, *J. Power Sources* 146 (2005) 473.
- [10] S.J. Lee, H.Y. Lee, S.H. Jeong, H.K. Baik, S.M. Lee, *J. Power Sources* 111 (2002) 345.
- [11] N. Tamura, R. Ohshita, M. Fujimoto, S. Fujitani, M. Kamino, I. Yonezu, *J. Power Sources* 107 (2002) 48.
- [12] N. Tamura, R. Ohshita, M. Fujimoto, M. Kamino, S. Fujitani, *J. Electrochem. Soc.* 150 (2003) A679.
- [13] C. Arbizzani, M. Lazzari, M. Mastragostino, *J. Electrochem. Soc.* 152 (2005) A289.
- [14] M. Yoshio, T. Tsumura, N. Dimov, *J. Power Sources* 146 (2005) 10.
- [15] M.S. Yazici, D. Krassowski, J. Prakash, *J. Power Sources* 141 (2005) 171.
- [16] H.C. Shin, J. Dong, M.L. Liu, *Adv. Mater.* 15 (2003) 1610.
- [17] H.C. Shin, M.L. Liu, *Chem. Mater.* 16 (2004) 5460.
- [18] J.W. Long, B. Dunn, D.R. Rolison, H.S. White, *Chem. Rev.* 104 (2004) 4463.
- [19] S. Yang, P.Y. Zavalij, M. Stanley Whittingham, *Electrochem. Commun.* 5 (2003) 587.
- [20] L.Y. Beaulieu, S.D. Beattie, T.D. Hatchard, J.R. Dahn, *J. Electrochem. Soc.* 150 (2003) A419.
- [21] J. Yang, M. Winter, J.O. Besenhard, *Solid State Ionics* 90 (1996) 281.